

REVIEW

Open Access



# Graphene nanoribbons: current status, challenges and opportunities

Shuo Lou<sup>1,2,3</sup>, Bosai Lyu<sup>1,2,3</sup>, Xianliang Zhou<sup>1,2,3</sup>, Peiyue Shen<sup>1,2,3</sup>, Jiajun Chen<sup>1,2,3</sup> and Zhiwen Shi<sup>1,2,3\*</sup>

## Abstract

Graphene nanoribbons (GNRs) are narrow strips of graphene with widths ranging from a few nanometers to a few tens of nanometers. GNRs possess most of the excellent properties of graphene, while also exhibiting unique physical characteristics not found in graphene, such as an adjustable band gap and spin-polarized edge states. These properties make GNRs an appealing candidate for carbon-based electronics. In this review, we begin by introducing the edge geometry and electronic bands of GNRs. We then discuss various methods for fabricating GNRs and analyze the characteristics of each method. Subsequently, the performance of GNR field-effect transistor devices obtained from a few representative GNR fabrication methods is discussed and compared. We also investigate the use of GNRs as quantum dots and spintronic devices. Finally, the challenges and opportunities of GNRs as a quantum material for next-generation electronics and spintronics are explored and proposed.

**Keywords:** Graphene nanoribbons, Fabrication methods, Field-effect transistor device, Quantum dots, Spintronic devices

## 1 Introduction

Ever since the discovery of graphene in 2004, a single layer of carbon atoms arranged in a honeycomb pattern, its exceptional properties in terms of electronics, mechanics, and heat conductivity have made it a highly promising material for various applications [1–12]. However, its lack of a bandgap structure has limited its potential for use in electronics. Graphene nanoribbons (GNRs) which are narrow strips of graphene with nanometer-scale widths, have attracted significant attention in the fields of nanotechnology and materials science due to their unique properties [13–16]. One outstanding feature of GNRs is their ability to possess a bandgap, unlike pristine graphene. By adjusting the width and edge configurations of nanoribbons, their electronic properties can be finely tuned, allowing for

the creation of semiconducting behavior. This tunability makes GNRs highly promising for applications in electronics, such as transistors, sensors, and even quantum dots [17–25]. In light of this, great efforts have been devoted to the study of GNRs.

Here, we will review the methods developed for fabricating GNRs and their potential applications. We will first briefly summarize the relationship between the edge types and band structure of GNRs, and then provide an overview of the main fabrication methods, categorized as top-down and bottom-up approaches. The progress of GNRs in field-effect transistors, quantum dot, and spintronic devices is also discussed. Furthermore, we will briefly discuss the challenges and opportunities in this rapidly developing field.

## 2 Edge types and electronic band structure of GNRs

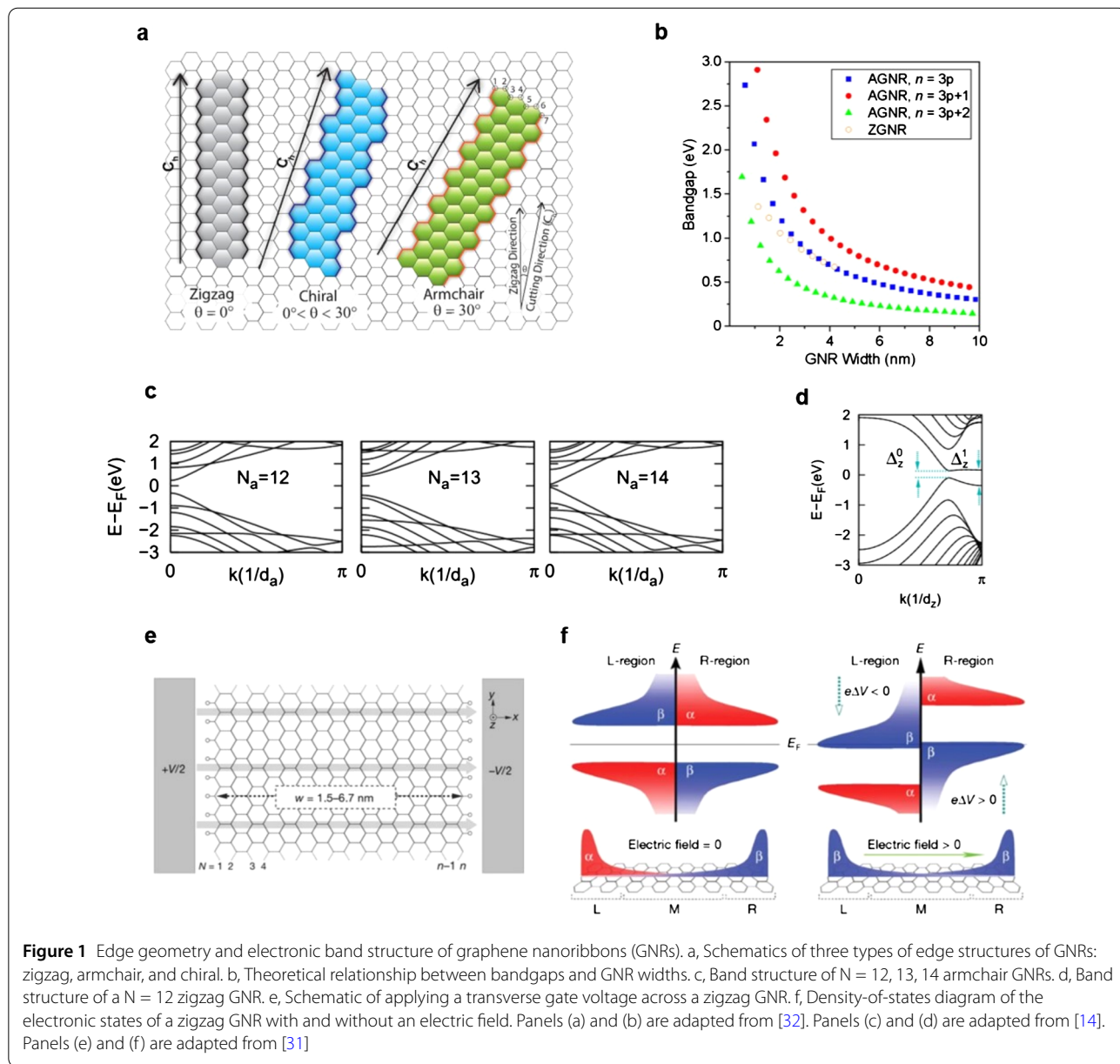
GNRs are narrow strips of graphene that have two long edges. Based on the edge geometry, GNRs can be classified into three types: armchair GNRs, zigzag GNRs, and chiral GNRs, as illustrated in Fig. 1(a). Armchair GNRs have

\*Correspondence: [zwshi@sjtu.edu.cn](mailto:zwshi@sjtu.edu.cn)

<sup>1</sup>Key Laboratory of Artificial Structures and Quantum Control (Ministry of Education), Shenyang National Laboratory for Materials Science, School of Physics and Astronomy, Shanghai Jiao Tong University, Shanghai 200240, China

<sup>2</sup>Collaborative Innovation Centre of Advanced Microstructures, Nanjing University, Nanjing 210093, China

Full list of author information is available at the end of the article

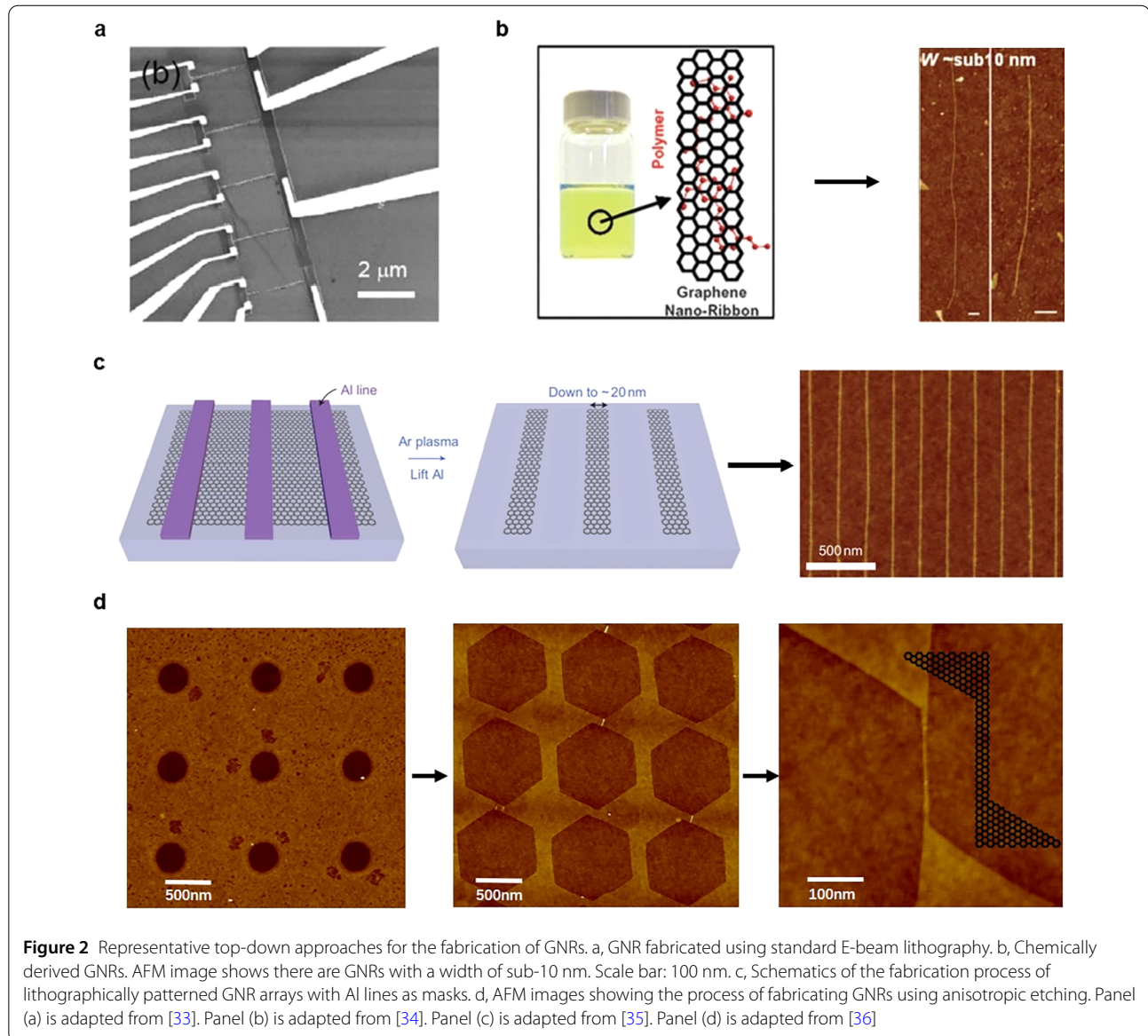


edges with an armchair shape, while zigzag GNRs have edges with a zigzag shape. GNRs with other edge structures are referred to as chiral GNRs.

The properties of GNRs highly rely on their edge types. Early tight-binding calculations predicted that armchair GNRs exhibit either a metallic or semiconducting band structure, depending on their widths [13, 26–28]. Specifically, an armchair GNR is metallic if  $N = 3p + 2$  (where  $N$  is the number of dimer lines across the ribbon and  $p$  is a positive integer). Otherwise, it is semiconducting. Recent ab-initio calculations have shown that all armchair GNRs actually exhibit semiconducting behavior [14, 16]. The bandgap of an armchair GNR is inversely proportional to its width and falls into three categories, with a hierarchy

of gap size represented by  $\Delta_{(3p+1)} > \Delta_{3p} > \Delta_{(3p+2)}$ , as shown in Fig. 1(b) and (c). The presence of energy gaps in armchair GNRs is a result of both quantum confinement and the significant influence of the edges.

Early tight-binding calculations predicted that all zigzag GNRs are metallic, exhibiting a flat band with a high density of states at zero energy, as well as peculiar edge states on both sides of the ribbon, regardless of their widths [13, 26–28]. However, recent ab-initio calculations have shown that the flat band observed in the tight-binding calculation is not stable when considering spin splitting [14]. It is now predicted that zigzag GNRs have a magnetic insulating ground state, with ferromagnetic ordering at each zigzag edge and anti-ferromagnetism across the ribbon



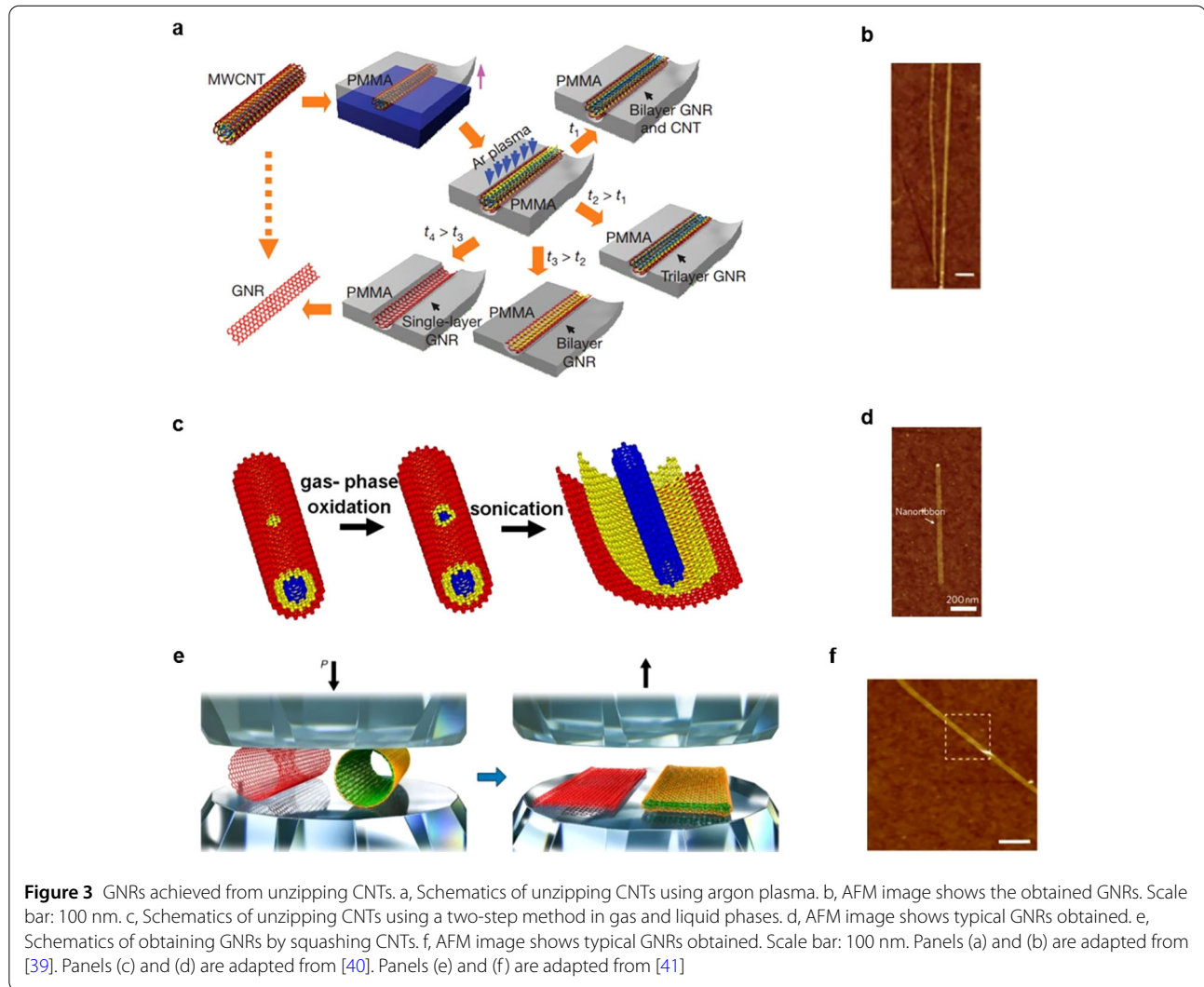
[14, 29, 30] (Fig. 1(d)). By applying an in-plane transverse electric field, it is expected that zigzag GNRs can exhibit half-metallicity by altering energy levels and eliminating the degeneracy of spin states [31] (Fig. 1(e) and (f)).

### 3 Top-down approaches: cutting graphene into GNRs

The synthesis of GNRs forms the basis for their use in electronic applications. In the past decades, various methods have been developed to create these nanoribbons. These methods can be divided into two categories: top-down and bottom-up.

Top-down methods refer to creating GNRs from graphene or carbon nanotubes. GNRs are essentially narrow stripes of graphene, which can be achieved by cutting

two-dimensional graphene into one-dimensional nanoribbons using various approaches. One way to fabricate GNRs is through top-down lithographic patterning of graphene sheets using electron-beam lithography combined with oxygen plasma etching [33] (Fig. 2(a)), and GNRs obtained this way are typically wider than 10 nm due to the limitation of lithography resolution. Another method involves a chemical route that can produce GNRs with a width below 10 nm. Commercial expandable graphite is first exfoliated by heating it to 1000°C in forming gas. The resulting exfoliated graphite is then dispersed in a polymer solution through sonication to form a homogeneous suspension. GNRs can be found in materials deposited on substrates from the supernatant [34] (Fig. 2(b)). GNR arrays can also be fabricated by lithographic patterning of graphene using



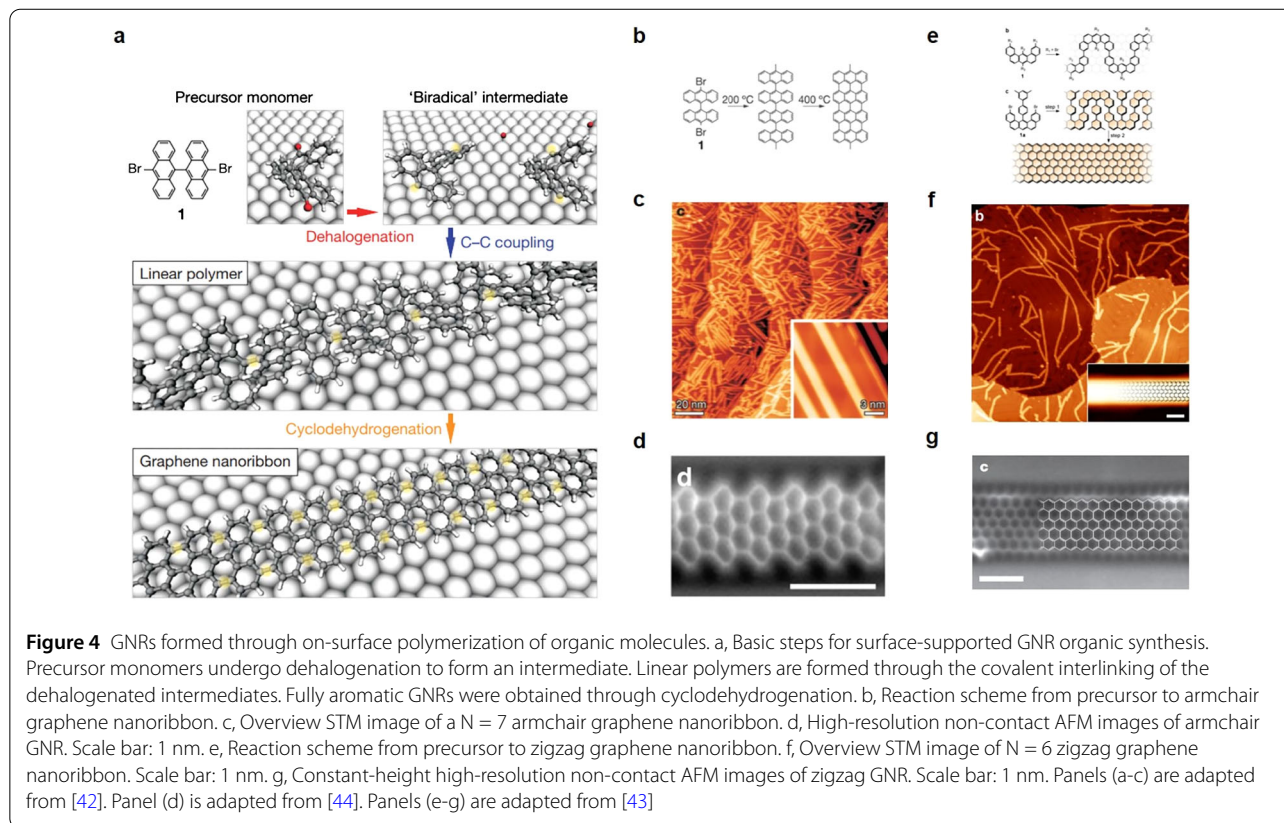
aluminum lines as a mask, followed by a gas-phase reaction to narrow the ribbons to a few nanometers in width [35] (Fig. 2(c)). Another approach, employing artificial defect patterning and hydrogen-plasma etching, can consistently achieve sub-10 nm wide GNRs with smooth zigzag edges [36] (Fig. 2(d)). Alternatively, GNRs with precisely controlled crystallographic edge orientations can be fabricated using scanning tunneling microscopy (STM) cutting [37]. However, the yield is extremely low. In addition, ultrathin GNRs can also be achieved through lithographic etching using nanomaterials as the etching mask, such as using nanowires and nanospheres [7, 38].

#### 4 Top-down approaches: unzipping carbon nanotubes

Longitudinal unzipping of carbon nanotubes (CNTs) is another common top-down method used to obtain GNRs with a very narrow width (< 10 nm). This can be achieved

through a masked gas-phase plasma etching process. The CNTs are first deposited onto a silicon substrate and then coated with a PMMA film. The PMMA-MWCNT film is then peeled off the substrate, flipped over, and exposed to an argon plasma. By adjusting the etching time, tri-, bi-, and single-layer GNRs can be produced [39] (Fig. 3(a) and (b)). Another method for unzipping CNTs involves a two-step process in both gas and liquid phases. In the mild gas-phase oxidation step, oxygen reacts with pre-existing defects on nanotubes, resulting in the formation of pits on the sidewalls. In the following solution-phase sonication step, the pits are enlarged and the tubes are unzipped using sonochemistry and hot gas bubbles [40] (Fig. 3(c) and (d)). GNRs can also be obtained by compressing CNTs using a diamond anvil cell. Under high-pressure and thermal treatment, CNTs are compressed and collapsed, forming closed-edge GNRs [41] (Fig. 3(e) and (f)). Edge-opened GNRs can be obtained by etching the edges using  $\text{HNO}_3$ .





## 5 Bottom-up approaches: on-surface polymerization

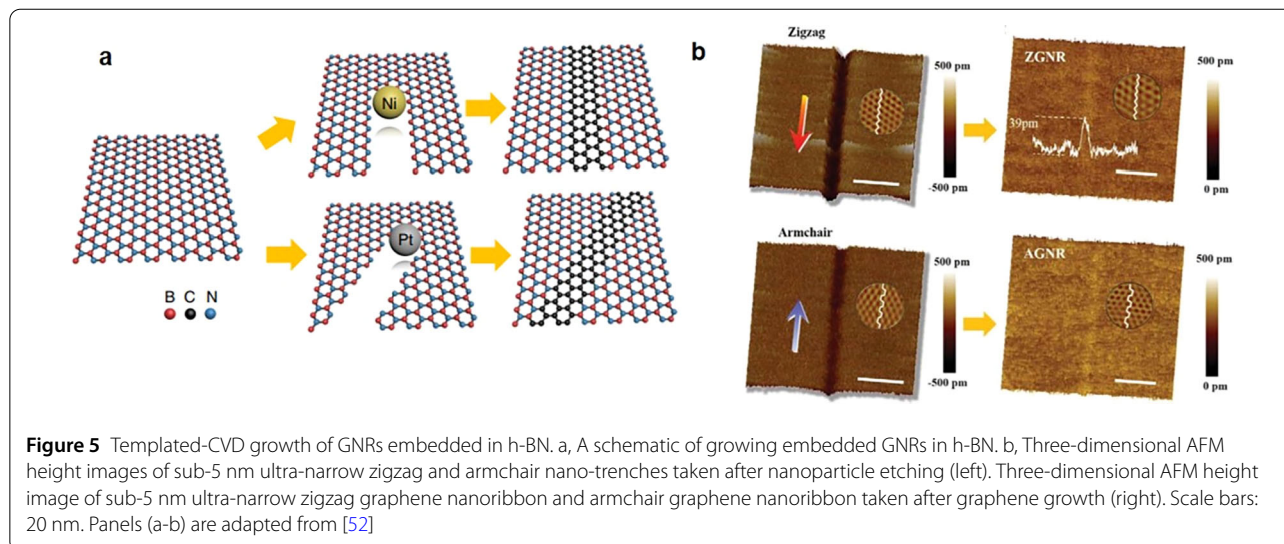
In order to create narrow GNRs with smooth edges, another synthetic route for GNRs called bottom-up was developed. Bottom-up methods include various approaches, such as the polymerization of organic molecules on metal substrates [42–44], epitaxy on SiC nanofacets [45, 46], synthesis using nickel nanobar [46–48], chemical vapor deposition (CVD) on Germanium substrates [49, 50], catalyzed CVD templated growth on hexagonal boron nitride (h-BN) [51, 52] and metal nanoparticle catalyzed CVD on h-BN substrates [53, 54].

On-surface polymerization is a bottom-up method for producing atomically precise GNRs of various topologies and widths. The process involves coupling or polymerizing specific organic monomers to synthesize atomically precise GNRs on the metal surface. The topology, width, and edge periphery of GNRs are defined by the structure of the precursor organic monomers, so a wide range of GNRs with different structure are accessible using this method. Figure 4(a) shows the typical process for creating armchair GNRs [42]. Firstly, precursor monomers undergo dehalogenation to form an intermediate product. The dehalogenated intermediates then diffuse along the surface and form single covalent C–C bonds between each monomer, resulting in polymer chains when annealed at 200°C. Fi-

nally, annealing the sample at 400°C induces intramolecular cyclodehydrogenation of the polymer chain to form an  $N = 7$  armchair ribbon. By employing a similar process of surface-assisted polymerization and subsequent cyclization, suitably designed U-shaped molecular precursors can be used to synthesize zigzag GNRs [43]. Figure 4(b) and (e) are simplified reaction schemes from precursors to armchair and zigzag GNRs. The STM images in Fig. 4(c) and (f) show the straight structure of both armchair and zigzag GNRs on Au surface. Constant-height, high-resolution, non-contact AFM images in Fig. 4(d) and (g) show atomically precise armchair and zigzag edge structures of the synthesized GNRs.

## 6 Bottom-up approaches: templated-CVD growth

The method of templated CVD growth on h-BN can control over the chirality of monolayer GNRs directly embedded in h-BN nano-trenches [51, 52]. This growth method can be divided into two steps: etching trenches in h-BN and growing GNRs embedded in the trenches (Fig. 5(a)). Metal nanoparticles, such as nickel and platinum, are used for catalytically etching the h-BN substrate, resulting in trenches with specific orientations. Nickel (Ni) nanoparticles create trenches aligned along the zigzag direction of h-BN, while platinum (Pt) nanoparticles form trenches along the armchair direction. Subsequently, the trenches



were filled with GNRs using gaseous catalyzed CVD. GNRs with zigzag or armchair edges embedded in h-BN were achieved using Ni or Pt nanoparticles, respectively (Fig. 5(b)). The lateral connectivity between the GNRs and h-BN allows for the creation of in-plane heterostructures with lattice coherence.

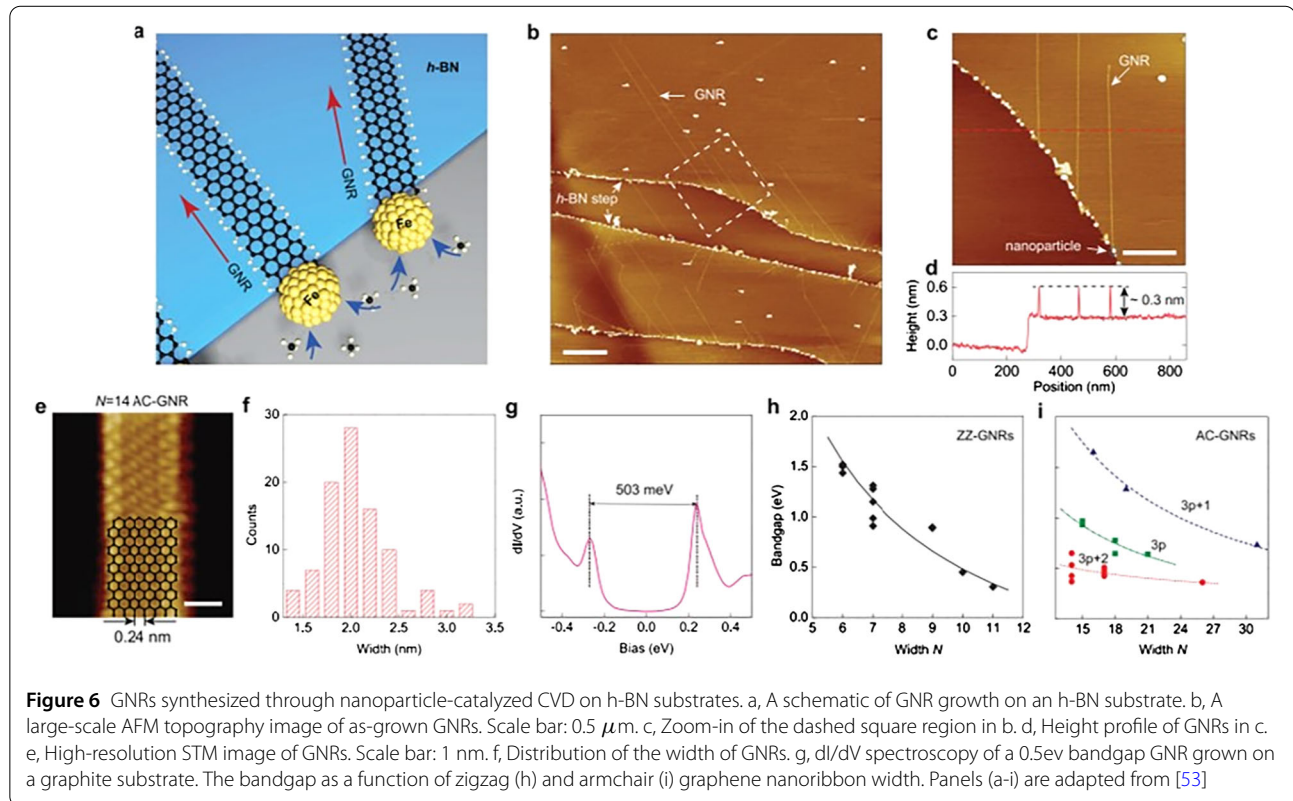
## 7 Bottom-up approaches: nanoparticle-catalyzed CVD growth

In the past, metal-nanoparticle catalyzed CVD has been commonly used to grow carbon nanotubes. Recently, a new method has been developed where micrometer-long, high-quality narrow graphene nanoribbons (GNRs) can be directly synthesized on insulating h-BN substrates using metal nanoparticle-catalyzed CVD [53]. This approach presents a significant advancement in the efficient growth of GNRs (Fig. 6(a-d)). For the first time, the elongated nanoribbons have been grown directly on top of an insulating h-BN substrate, which is a crucial step for their potential application in field-effect electronic and spintronic devices. The as-grown GNRs can reach lengths of up to 10  $\mu\text{m}$  and have a uniform thickness of one layer. This generic growth method also allows for the growth of GNRs on a graphite substrate, which enables further characterization using STM. STM results have shown the smooth armchair edge of the GNRs (Fig. 6(e)). The width distribution of GNRs was measured using STM, and the average width of GNRs was found to be around 2 nm, limited by the size of the nanoparticles (Fig. 6(f)). Scanning tunneling spectroscopy (STS) results of the GNRs fabricated using this approach clearly demonstrate that these systems have controllable bandgaps that strongly depend on their width, in agreement with theoretical predictions (Fig. 6(g-i)). For armchair GNRs, experimental observations have shown that the bandgap is inversely proportional to the

width and falls into three categories ( $N = 3p, 3p + 1, 3p + 2$ ) (refer to Fig. 6(i)).

This method can be considered a generic approach for growing both GNRs and CNTs. The ratio of GNRs to CNTs can be arbitrarily tuned by changing the growth temperature or hydrogen partial pressures. This allows for the selective production of pure GNRs, pure CNTs, or a mixture of GNRs and CNTs with a desired population ratio (Fig. 7(e)). The tunability of the generic growth is well explained by a competing nucleation theory. The nucleation of GNRs or CNTs by catalysts is determined by the free energy involved in their formation, which is controlled by the growth temperature and atmosphere. Planar GNRs have a larger contact area with the substrate compared to tubular CNTs, and therefore have larger van der Waals adhesion (Fig. 7(a)). The free energy of formation for CNTs and GNRs takes into account various factors, including curvature energy, H-passivated edge energy, and van der Waals adhesion (Fig. 7(b)). The calculation results show that the free energy of GNRs changes systematically with the growth temperature and hydrogen pressure, due to the corresponding change in edge formation energy (Fig. 7(c)). A phase diagram of nucleation of GNRs versus CNTs is drawn based on the free energy calculations. Both the experimental and theoretical results show that lower temperatures and higher hydrogen pressures favor the growth of GNRs, while higher temperatures and lower hydrogen pressures support the growth of CNTs (Fig. 7(d)).

Under the guidance of the theory, the growth of GNR/CNT intramolecular junctions was successfully achieved by changing the  $\text{H}_2$  partial pressures during a single growth process [54] (Fig. 7(f) and (g)). The obtained GNR/CNT heterojunction has potential applications as fundamental components for future carbon-based electronic and optoelectronic devices, such as field-effect transistors,



logic gates, and high-performance photodetectors. This method provides a scalable fabrication technique for producing micrometer-long high-quality ultranarrow GNRs on insulating h-BN substrates, which is crucial for the further utilization of GNRs in nanoelectronic devices.

## 8 GNRs-based devices

GNRs have excellent electronic properties, including high carrier mobility, which they inherit from graphene. Additionally, GNRs have a finite bandgap, making them attractive for future nanoelectronics. The electronic properties of GNRs, such as band gap and carrier mobility, depend largely on their edge type, edge smoothness, and ribbon width. The choice of fabrication methods significantly impacts the structure and quality of GNRs. Field-effect transistor (FET) devices were used to test the electronic performance of GNRs, such as carrier mobility and on/off ratios.

GNRs formed through lithographic patterning of graphene can be further narrowed by controlled etching. The GNR FET device with a width  $\sim 4 \text{ nm}$  exhibited ambipolar transport in air, with an on/off ratio  $> 1 \times 10^4$ , clear evidence of bandgap opening through lateral quantum confinement [33]. It was also observed that as the width decreases, the on/off ratio increases. A similar relationship between the on/off ratio and the width of GNRs was observed in GNRs obtained through unzipping CNTs [39, 40, 55]. The mobilities of the GNRs made by both

methods were also similar, approximately 10 times lower than those of large two-dimensional graphene sheets. The difference in mobility is likely due to edge scattering in the GNRs. FET devices fabricated using GNRs derived from sonochemical exfoliation of graphite exhibited on/off ratios of approximately 1, 5, 100, and greater than  $10^4$  [5] for GNR widths of  $50 \text{ nm}$ ,  $20 \text{ nm}$ ,  $10 \text{ nm}$ , and sub- $10 \text{ nm}$ , respectively [34] (Fig. 8(a)). Notably, all sub- $10 \text{ nm}$  GNRs exhibit an on/off ratio greater than  $10^4$  [5] (Fig. 8(c)). Analysis based on electrostatic simulations of gate capacitances led to an estimated hole mobility of approximately  $100$  to  $200 \text{ cm}^2 \text{ V}^{-1} \text{ s}^{-1}$  in the sub- $10 \text{ nm}$  width GNRs.

GNRs obtained through bottom-up on-surface synthesis of organic molecules need to be transferred onto an insulating surface in order to subsequently fabricate GNR-FET device.  $N = 9$  armchair GNR-FETs fabricated by this method exhibited [17] on-current  $I_{\text{on}} > 1 \mu\text{A}$  and an on/off ratio  $\sim 10^4$  [5]. Templated-CVD GNRs embedded in h-BN trenches have high field-effect mobilities  $\sim 1500 \text{ cm}^2 \text{ V}^{-1} \text{ s}^{-1}$  and an on/off ratio  $\sim 10^4$  [5] for sub- $10 \text{ nm}$  GNR devices [52] (Fig. 8(b) and (d)). The scattering mean free path in these narrow GNRs was estimated to be around  $50 \text{ nm}$  (Fig. 8(d)).

In addition to traditional field-effect transistors, GNRs can also be used to create quantum dot devices, which are important for quantum computing applications. GNRs exhibit specific quantum transport phenomena, such as



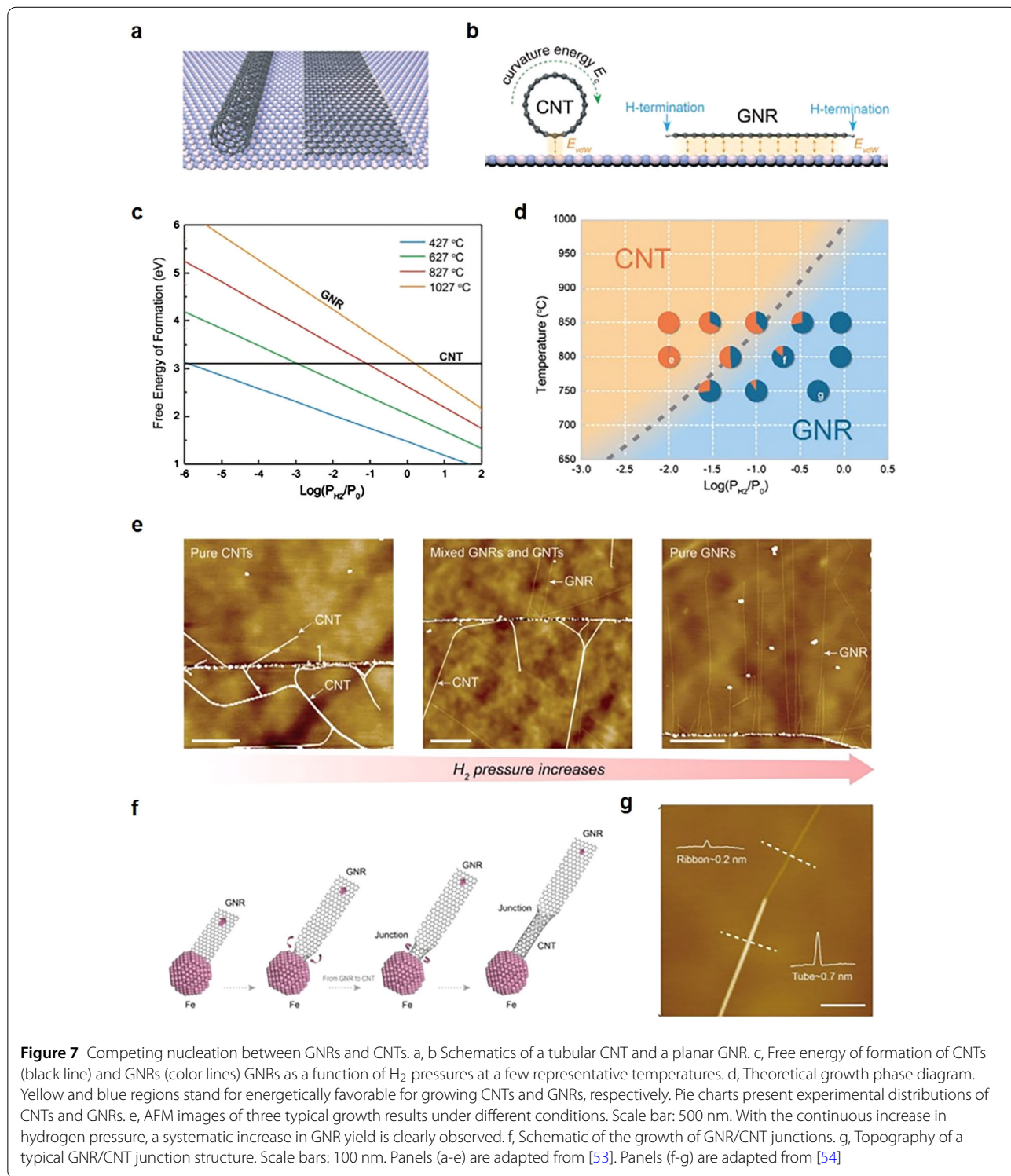


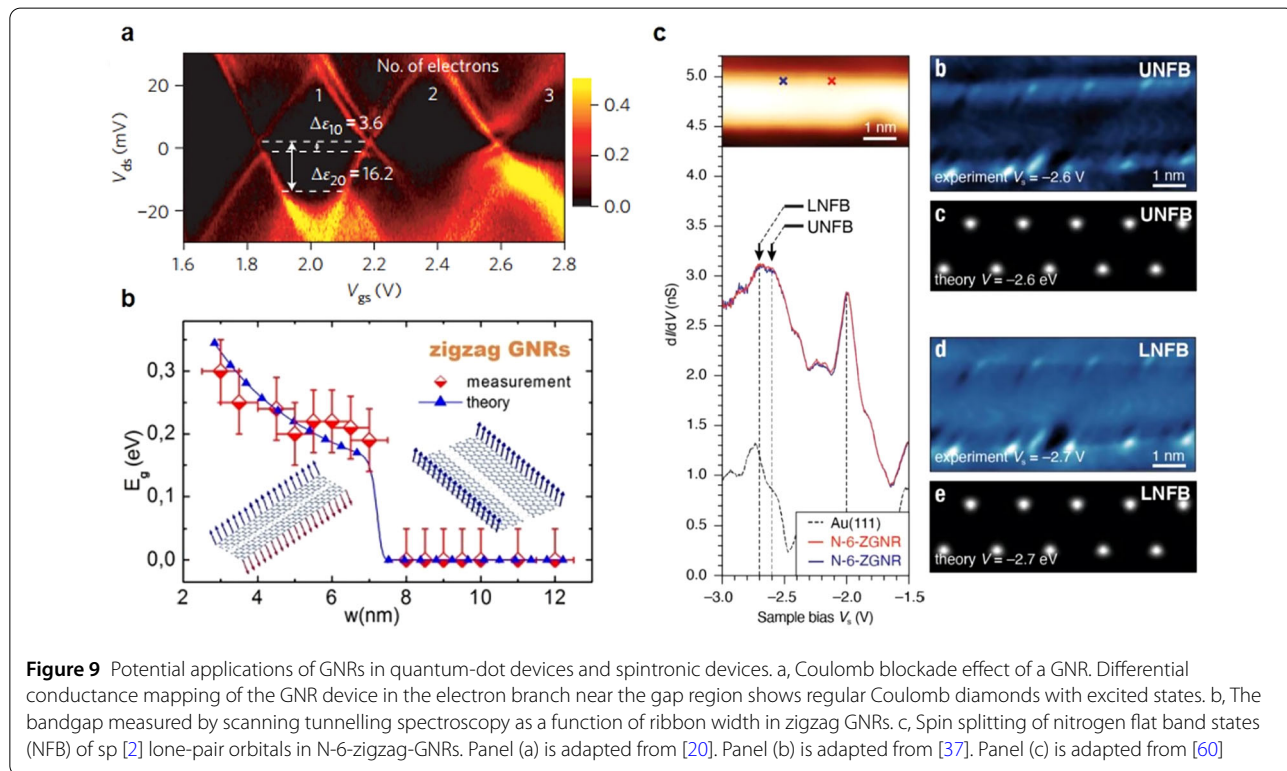
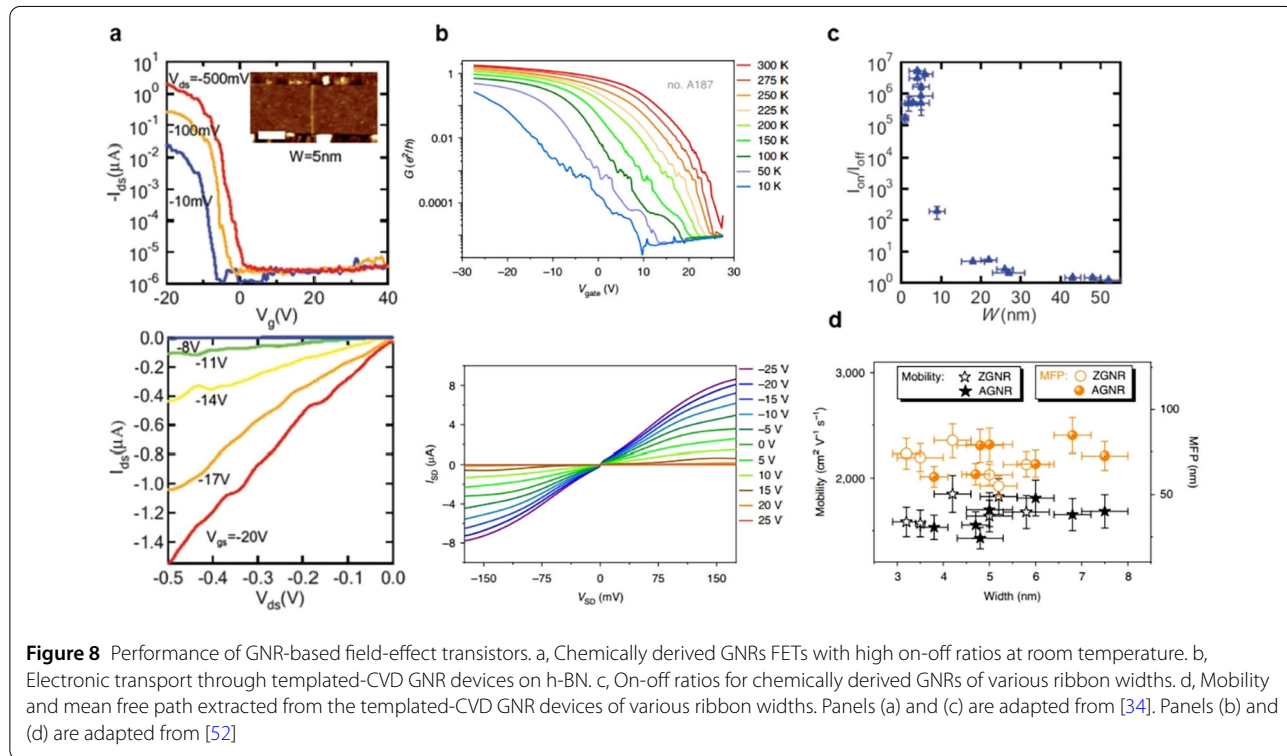
**Figure 7** Competing nucleation between GNRs and CNTs. a, b Schematics of a tubular CNT and a planar GNR. c, Free energy of formation of CNTs (black line) and GNRs (color lines) GNRs as a function of  $H_2$  pressures at a few representative temperatures. d, Theoretical growth phase diagram. Yellow and blue regions stand for energetically favorable for growing CNTs and GNRs, respectively. Pie charts present experimental distributions of CNTs and GNRs. e, AFM images of three typical growth results under different conditions. Scale bar: 500 nm. With the continuous increase in hydrogen pressure, a systematic increase in GNR yield is clearly observed. f, Schematic of the growth of GNR/CNT junctions. g, Topography of a typical GNR/CNT junction structure. Scale bars: 100 nm. Panels (a-e) are adapted from [53]. Panels (f-g) are adapted from [54]

Coulomb blockade and the Kondo effect [56–59]. Short-length narrow GNRs can be seen as graphene quantum dots and potentially be suitable for single-electron transistors. High-quality GNRs could behave like a single quantum dot at low temperature with well-defined Coulomb

blockade diamonds, allowing for distinguishing the excited states and counting the tunnelling electrons and holes for quantum transport study [20] (Fig. 9(a)).

Zigzag GNRs have the potential to be used as spintronic devices because of their predicted magnetic order. In spin-





tronic devices, the spin of an electron is as important as its charge for storing information and performing logic operations. The unique magnetism of zigzag GNRs is a result of the topological properties of graphene, which induce localized electronic states along the edges of the ribbon. The spins of these states are aligned if they are on the same edge, and they have antiparallel alignment if they are on opposite edges. Using a nanofabrication technique based on STM etching, GNRs with precise zigzag edges and controlled widths have been achieved. Upon increasing the width of zigzag ribbons, a transition from semiconductor to metal is observed. This transition indicates a change in the magnetic coupling between the opposite edges from an antiferromagnetic to a ferromagnetic configuration [37] (Fig. 9(b)). To confirm the magnetism of zigzag GNRs, special GNRs with nitrogen atoms replacing some carbon atoms along the edges were synthesized. The inclusion of nitrogen stabilizes the zigzag edges and allows for the investigation of their unconventional magnetism. Calculations and spectroscopy reveal a significant spin splitting of low-lying nitrogen bands induced by the ferromagnetically ordered edge states of zigzag GNRs, providing evidence for the predicted emergent magnetic order [60] (Fig. 9(c)).

However, almost all experimental evidence for the spin-polarized edges in zigzag GNRs so far seems to be indirect, and practical spintronic devices based on zigzag GNRs have not yet been realized. There are challenges in directly confirming the magnetism of zigzag GNRs in experiments. The magnetic properties of zigzag GNRs are highly dependent on the specific arrangement of atoms at the edges. Currently, the most successful method for synthesizing atomically precise zigzag GNRs is through on-surface polymerization of organic molecules. However, GNRs produced using this method are very short and are on a conductive metal substrate, making them unsuitable for device fabrication. Additionally, zigzag GNRs are easily oxidized and chemically unstable in air. Presumably, encapsulated GNRs with atomically precise zigzag edges would be ideal for creating GNR-based spintronic devices.

## 9 Summary and perspective

In this review paper, we start with introducing the edge structure and band structure of GNRs. Then, we provide an overview of the current methods for fabricating GNRs, categorizing them into top-down and bottom-up approaches, and discussing a few representative methods in depth. The potential applications of GNRs in field-effect transistors, quantum dots, and spintronic devices are also discussed.

Reviewing the development of GNRs in recent decades, there are still numerous challenges and opportunities in the fabrication methods and application of GNRs. One major challenge is the inability of current fabrication

methods to produce high-quality GNRs with precise control over their length, layers, edge structure, and arrangement. Additionally, the transfer process required for device fabrication often leads to contamination, which has a negative impact on device performance. However, the use of h-BN as a substrate for synthesizing GNRs shows promise for high-performance devices. This approach eliminates the need for transfer during fabrication and improves the electrical performance of graphene devices. Growing GNRs between h-BN layers provides natural encapsulation during the growth process, protecting them from contamination and offering advantages for creating extremely high-performance GNR devices. Furthermore, there are opportunities to discover novel physical phenomena in GNRs, such as the one-dimensional Luttinger liquid behavior [61]. As one-dimensional moiré patterns have been observed in GNRs grown on h-BN substrates, it is worth exploring how the superlattice structure affects GNR properties, especially the Luttinger liquid behavior. It is believed that further exploration of GNRs will lead to significant progress and offer practical solutions for carbon-based high-performance electronic devices.

### Acknowledgements

Not applicable.

### Funding

This work was supported by the National Natural Science Foundation of China (Nos. 12074244 and 12374292), the National Key R&D Program of China (No. 2021YFA1202902), and the open research fund of Songshan Lake Materials Laboratory (No. 2021SLABFK07).

### Data availability

Not applicable.

## Declarations

### Ethics approval and consent to participate

Not applicable.

### Consent for publication

Not applicable.

### Competing interests

The authors declare no competing interests.

### Author contributions

SL, BL and ZS conceived the project. XZ summarized edge types and electronic band structure of GNRs. PS and JC summarized GNRs-based devices part. SL and ZS wrote the paper with input from all authors. All authors discussed the results and commented on the manuscript. All authors read and approved the final manuscript.

### Author details

<sup>1</sup>Key Laboratory of Artificial Structures and Quantum Control (Ministry of Education), Shenyang National Laboratory for Materials Science, School of Physics and Astronomy, Shanghai Jiao Tong University, Shanghai 200240, China. <sup>2</sup>Collaborative Innovation Centre of Advanced Microstructures, Nanjing University, Nanjing 210093, China. <sup>3</sup>Tsung-Dao Lee Institute, Shanghai Jiao Tong University, Shanghai 200240, China.

Received: 15 November 2023 Revised: 3 February 2024

Accepted: 8 February 2024 Published online: 20 February 2024

## References

- Novoselov KS et al (2004) Electric field effect in atomically thin carbon films. *Science* 306:666–669. <https://doi.org/10.1126/science.1102896>
- Zhang YB, Tan YW, Stormer HL, Kim P (2005) Experimental observation of the quantum Hall effect and Berry's phase in graphene. *Nature* 438:201–204. <https://doi.org/10.1038/nature04235>
- Novoselov KS et al (2005) Two-dimensional gas of massless Dirac fermions in graphene. *Nature* 438:197–200. <https://doi.org/10.1038/nature04233>
- Berger C et al (2006) Electronic confinement and coherence in patterned epitaxial graphene. *Science* 312:1191–1196. <https://doi.org/10.1126/science.1125925>
- Wang F et al (2008) Gate-variable optical transitions in graphene. *Science* 320:206–209. <https://doi.org/10.1126/science.1152793>
- Lin YM et al (2010) 100-GHz transistors from wafer-scale epitaxial graphene. *Science* 327:662–662. <https://doi.org/10.1126/science.1184289>
- Liao L et al (2010) High-speed graphene transistors with a self-aligned nanowire gate. *Nature* 467:305–308. <https://doi.org/10.1038/nature09405>
- Balandin AA et al (2008) Superior thermal conductivity of single-layer graphene. *Nano Lett* 8:902–907. <https://doi.org/10.1021/nl0731872>
- Cai W et al (2010) Thermal transport in suspended and supported monolayer graphene grown by chemical vapor deposition. *Nano Lett* 10:1645–1651. <https://doi.org/10.1021/nl9041966>
- Chen S et al (2012) Thermal conductivity of isotopically modified graphene. *Nat Mater* 11:203–207. <https://doi.org/10.1038/nmat3207>
- Lee C, Wei X, Kysar JW, Hone J (2008) Measurement of the elastic properties and intrinsic strength of monolayer graphene. *Science* 321:385–388. <https://doi.org/10.1126/science.1157996>
- Raju APA et al (2014) Wide-area strain sensors based upon graphene-polymer composite coatings probed by Raman spectroscopy. *Adv Funct Mater* 24:2865–2874. <https://doi.org/10.1002/adfm.201302869>
- Nakada K, Fujita M, Dresselhaus G, Dresselhaus MS (1996) Edge state in graphene ribbons: nanometer size effect and edge shape dependence. *Phys Rev B* 54:17954–17961. <https://doi.org/10.1103/PhysRevB.54.17954>
- Son Y-W, Cohen ML, Louie SG (2006) Energy gaps in graphene nanoribbons. *Phys Rev Lett* 97. <https://doi.org/10.1103/PhysRevLett.97.216803>
- Betti A, Fiori G, Iannaccone G (2011) Drift velocity peak and negative differential mobility in high field transport in graphene nanoribbons explained by numerical simulations. *Appl Phys Lett* 99. <https://doi.org/10.1063/1.3664091>
- Barone V, Hod O, Scuseria GE (2006) Electronic structure and stability of semiconducting graphene nanoribbons. *Nano Lett* 6:2748–2754. <https://doi.org/10.1021/nl0617033>
- Llinas JP et al (2017) Short-channel field-effect transistors with 9-atom and 13-atom wide graphene nanoribbons. *Nat Commun* 8. <https://doi.org/10.1038/s41467-017-00734-x>
- Wang X et al (2008) Room-temperature all-semiconducting sub-10-nm graphene nanoribbon field-effect transistors. *Phys Rev Lett* 100. <https://doi.org/10.1103/PhysRevLett.100.206803>
- Li H et al (2021) Photoluminescent semiconducting graphene nanoribbons via longitudinally unzipping single-walled carbon nanotubes. *ACS Appl Mater Interfaces* 13:52892–52900. <https://doi.org/10.1021/acsmi.1c14597>
- Wang X et al (2011) Graphene nanoribbons with smooth edges behave as quantum wires. *Nat Nanotechnol* 6:563–567. <https://doi.org/10.1038/nnano.2011.138>
- Lin M-W et al (2011) Approaching the intrinsic band gap in suspended high-mobility graphene nanoribbons. *Phys Rev B* 84. <https://doi.org/10.1103/PhysRevB.84.125411>
- Lu X et al (2016) Graphene nanoribbons epitaxy on boron nitride. *Appl Phys Lett* 108. <https://doi.org/10.1063/1.4943940>
- Schwierz F (2010) Graphene transistors. *Nat Nanotechnol* 5:487–496. <https://doi.org/10.1038/nnano.2010.89>
- Johnson JL, Behnam A, Pearton SJ, Ural A (2010) Hydrogen sensing using Pd-functionalized multi-layer graphene nanoribbon networks. *Adv Mater* 22:4877. <https://doi.org/10.1002/adma.201001798>
- Pour MM et al (2017) Laterally extended atomically precise graphene nanoribbons with improved electrical conductivity for efficient gas sensing. *Nat Commun* 8. <https://doi.org/10.1038/s41467-017-00692-4>
- Fujita M, Wakabayashi K, Nakada K, Kusakabe K (1996) Peculiar localized state at zigzag graphite edge. *J Phys Soc Jpn* 65:1920–1923. <https://doi.org/10.1143/jpsj.65.1920>
- Wakabayashi K, Fujita M, Ajiki H, Sigrist M (1999) Electronic and magnetic properties of nanographite ribbons. *Phys Rev B* 59:8271–8282. <https://doi.org/10.1103/PhysRevB.59.8271>
- Ezawa M (2006) Peculiar width dependence of the electronic properties of carbon nanoribbons. *Phys Rev B* 73. <https://doi.org/10.1103/PhysRevB.73.045432>
- Palacios JJ, Fernandez-Rossier J, Brey L (2008) Vacancy-induced magnetism in graphene and graphene ribbons. *Phys Rev B* 77. <https://doi.org/10.1103/PhysRevB.77.195428>
- Fernandez-Rossier J (2008) Prediction of hidden multiferroic order in graphene zigzag ribbons. *Phys Rev B* 77. <https://doi.org/10.1103/PhysRevB.77.075430>
- Son Y-W, Cohen ML, Louie SG (2006) Half-metallic graphene nanoribbons. *Nature* 444:347–349. <https://doi.org/10.1038/nature05180>
- Saraswat V, Jacobberger RM, Arnold MS (2021) Materials science challenges to graphene nanoribbon electronics. *ACS Nano* 15:3674–3708. <https://doi.org/10.1021/acsnano.0c07835>
- Han MY, Oezylmaz B, Zhang Y, Kim P (2007) Energy band-gap engineering of graphene nanoribbons. *Phys Rev Lett* 98. <https://doi.org/10.1103/PhysRevLett.98.206805>
- Li X, Wang X, Zhang L, Lee S, Dai H (2008) Chemically derived, ultrasmooth graphene nanoribbon semiconductors. *Science* 319:1229–1232. <https://doi.org/10.1126/science.1150878>
- Wang X, Dai H (2010) Etching and narrowing of graphene from the edges. *Nat Chem* 2:661–665. <https://doi.org/10.1038/nchem.719>
- Shi Z et al (2011) Patterning graphene with zigzag edges by self-aligned anisotropic etching. *Adv Mater* 23:3061. <https://doi.org/10.1002/adma.201100633>
- Magda GZ et al (2014) Room-temperature magnetic order on zigzag edges of narrow graphene nanoribbons. *Nature* 514:608. <https://doi.org/10.1038/nature13831>
- Liu L et al (2011) Nanosphere lithography for the fabrication of ultranarrow graphene nanoribbons and on-chip bandgap tuning of graphene. *Adv Mater* 23:1246. <https://doi.org/10.1002/adma.201003847>
- Jiao L, Zhang L, Wang X, Diankov G, Dai H (2009) Narrow graphene nanoribbons from carbon nanotubes. *Nature* 458:877–880. <https://doi.org/10.1038/nature07919>
- Jiao L, Wang X, Diankov G, Wang H, Dai H (2010) Facile synthesis of high-quality graphene nanoribbons. *Nat Nanotechnol* 5:321–325. <https://doi.org/10.1038/nnano.2010.54>
- Chen C et al (2021) Sub-10-nm graphene nanoribbons with atomically smooth edges from squashed carbon nanotubes. *Nat Electron* 4:653–663. <https://doi.org/10.1038/s41928-021-00633-6>
- Cai J et al (2010) Atomically precise bottom-up fabrication of graphene nanoribbons. *Nature* 466:470–473. <https://doi.org/10.1038/nature09211>
- Ruffieux P et al (2016) On-surface synthesis of graphene nanoribbons with zigzag edge topology. *Nature* 531:489. <https://doi.org/10.1038/nature17151>
- van der Lit J et al (2013) Suppression of electron-vibron coupling in graphene nanoribbons contacted via a single atom. *Nat Commun* 4. <https://doi.org/10.1038/ncomms3023>
- Sprinkle M et al (2010) Scalable templated growth of graphene nanoribbons on SiC. *Nat Nanotechnol* 5:727–731. <https://doi.org/10.1038/nnano.2010.192>
- Huang Q, Kim JJ, Ali G, Cho SO (2013) Width-tunable graphene nanoribbons on a SiC substrate with a controlled step height. *Adv Mater* 25:1144–1148. <https://doi.org/10.1002/adma.201202746>
- Suzuki H et al (2016) Wafer-scale fabrication and growth dynamics of suspended graphene nanoribbon arrays. *Nat Commun* 7. <https://doi.org/10.1038/ncomms11797>
- Kato T et al (2022) Scalable fabrication of graphene nanoribbon quantum dot devices with stable orbital-level spacing. *Commun Mater* 3. <https://doi.org/10.1038/s43246-022-00326-3>
- Jacobberger RM et al (2015) Direct oriented growth of armchair graphene nanoribbons on germanium. *Nat Commun* 6. <https://doi.org/10.1038/ncomms9006>
- Way AJ et al (2022) Graphene nanoribbons initiated from molecularly derived seeds. *Nat Commun* 13. <https://doi.org/10.1038/s41467-022-30563-6>
- Chen L et al (2017) Oriented graphene nanoribbons embedded in hexagonal boron nitride trenches. *Nat Commun* 8. <https://doi.org/10.1038/ncomms14703>



52. Wang HS et al (2021) Towards chirality control of graphene nanoribbons embedded in hexagonal boron nitride. *Nat Mater* 20:202. <https://doi.org/10.1038/s41563-020-00806-2>
53. Lyu B et al (2022) Catalytic growth of ultralong graphene nanoribbons on insulating substrates. *Adv Mater* 34. <https://doi.org/10.1002/adma.202200956>
54. Lou S et al (2023) Tunable growth of one-dimensional graphitic materials: graphene nanoribbons, carbon nanotubes, and nanoribbon/nanotube junctions. *Sci Rep* 13. <https://doi.org/10.1038/s41598-023-31573-0>
55. Kosynkin DV et al (2009) Longitudinal unzipping of carbon nanotubes to form graphene nanoribbons. *Nature* 458:872–875. <https://doi.org/10.1038/nature07872>
56. Sols F, Guinea F, Castro Neto AH (2007) Coulomb blockade in graphene nanoribbons. *Phys Rev Lett* 99. <https://doi.org/10.1103/PhysRevLett.99.166803>
57. Gallagher P, Todd K, Goldhaber-Gordon D (2010) Disorder-induced gap behavior in graphene nanoribbons. *Phys Rev B* 81. <https://doi.org/10.1103/PhysRevB.81.115409>
58. Stampfer C et al (2009) Energy gaps in etched graphene nanoribbons. *Phys Rev Lett* 102. <https://doi.org/10.1103/PhysRevLett.102.056403>
59. Goldhaber-Gordon D et al (1998) Kondo effect in a single-electron transistor. *Nature* 391:156–159. <https://doi.org/10.1038/34373>
60. Blackwell RE et al (2021) Spin splitting of dopant edge state in magnetic zigzag graphene nanoribbons. *Nature* 600:647. <https://doi.org/10.1038/s41586-021-04201-y>
61. Bockrath M et al (1999) Luttinger-liquid behaviour in carbon nanotubes. *Nature* 397:598–601. <https://doi.org/10.1038/17569>

## Publisher's Note

Springer Nature remains neutral with regard to jurisdictional claims in published maps and institutional affiliations.

Submit your manuscript to a SpringerOpen<sup>®</sup> journal and benefit from:

- ▶ Convenient online submission
- ▶ Rigorous peer review
- ▶ Open access: articles freely available online
- ▶ High visibility within the field
- ▶ Retaining the copyright to your article

---

Submit your next manuscript at ▶ [springeropen.com](https://www.springeropen.com)

---